one-photon resonant steps to sufficiently high levels at which electron-vibration coupling allows effective conversion of vibrational excitation to electronic excitation. The radiative decay of the electronic excitation then results in the observed luminescence. Our preliminary results indicate that MPE is effective only when it occurs via the vibrational ladder of SiH_x but not via the $OSiH_x$ stretch ladder.

There are substantial differences between the problem encountered with porous Si and the commonly studied MPE of polyatomic molecules. Each Si cluster consists of a large number ($\geq 10^6$) of Si atoms that form a core and a large number ($\sim 10^4$) of H atoms passivating its surface (*8*). The valence electrons in the nanocrystal are delocalized. The SiH_x stretch peaks in the vibrational spectrum are certainly inhomogeneously broadened, and their vibrational lifetimes could be much longer than the 8- to 25-ps pump pulsewidth used in our experiment. The higher excited states of the SiH_x vibrations should have shorter lifetimes. However, only when their lifetimes become shorter than the pump pulsewidth can they be considered to be effectively coupled with other vibrational modes of the system to form a quasi-continuum with a density of states that increases rapidly with energy. The observed I_{in}^5 dependence of the luminescence output from our porous Si sample at long excitation wavelengths suggests that the effective quasi-continuum starts at ~1.25 eV, because it takes a direct five-photon absorption of ~4.9-μm (0.25 eV) radiation to reach the quasi-continuum. An overall seven- to eight-photon absorption is needed to induce a single luminescent photon at 600 to 700 nm.

For the observed excitation spectra in Fig. 5, we offer the following explanation. The excitation spectrum, $F(\omega)$, of a five-photon excitation process up a vibrational ladder can be described by

$$F(\omega) = \int P(\{\gamma\}) \prod_{i=0}^{4} G_{i \rightarrow i+1}(\omega, \{\gamma\}) d\{\gamma\}$$

where ω is the angular frequency, $G_{i \rightarrow i+1}(\omega)$ is the homogeneous lineshape of the vibrational transition from $\upsilon = i$ to $\upsilon = i + 1$, $\{\gamma\}$ is a set of parameters describing the local environment, and $P(\{\gamma\})$ is the distribution function of $\{\gamma\}$. We expect the linewidth of $G_{i \rightarrow i+1}(\omega)$ to increase appreciably with the increase of i and pump intensity because of power broadening. If the vibrational anharmonicity is large, with only weak overlap between $G_{i \rightarrow i+1}(\omega)$ and $G_{i+1 \rightarrow i+2}(\omega)$, then the peak of $F(\omega)$ is dominated by $G_{0 \rightarrow 1}(\omega)$. This is the case for MPE at low pump intensities (Fig. 5). If with higher pump intensities, the overlap between $G_{i \rightarrow i+1}(\omega)$ and $G_{i+1 \rightarrow i+2}(\omega)$ due to power broadening becomes significant, then the peak of $F(\omega)$ should experience a red shift. This is the case of MPE via the vibrational modes at about 2110 cm^{-1} (Fig. 5). In the latter case, an alternative explanation is that the homogeneous linewidth is always larger than the anharmonic shift, but this is not likely considering that the known anharmonicity of SiH-stretch vibration for H/Si(111) is ~70 cm^{-1} (*12*).

We expect MPE-PL to be a generic process that could occur in many semiconductor clusters. Efficiency of MPE-PL via pumping up a vibrational ladder depends on the character of the vibrational mode and its coupling with the carrier excitation.

REFERENCES AND NOTES

1. Materials Research Society meetings in Boston and San Francisco and European Materials Research Society meeting in Strasbourg since 1991.
2. Aa. S. Sudbø, P. A. Schultz, E. R. Grant, Y. R. Shen, Y. T. Lee, *J. Chem. Phys.* **68**, 1306 (1978).
3. L. A. Bloomfield, M. E. Geusic, R. R. Freeman, W. L. Brown, *Chem. Phys. Lett.* **121**, 33 (1985).
4. R. I. McKay *et al.*, *J. Chem. Phys.* **95**, 1688 (1991).
5. See, for example, Y. R. Shen, *The Principles of Nonlinear Optics* (Wiley, New York, 1985), chap. 23.
6. J. Wang *et al.*, *Phys. Rev. Lett.* **69**, 3252 (1992).
7. X. Wang, in *Porous Silicon*, Z. Chuan and R. Tsu, Eds. (World Scientific, River Edge, NJ, 1994), pp. 77–98.
8. F. Koch, V. Petrova-Koch, T. Muschik, *J. Luminescence* **57**, 271 (1993).
9. T. Maruyama and S. Ohtani, *Appl. Phys. Lett.* **64**, 280 (1994).
10. The system generated 8-ps pulses at 20 Hz, tunable from 0.65 μm (15,400 cm^{-1}/1.9 eV) to 10 μm (1000 cm^{-1}/0.12 eV) with a linewidth of 2 cm^{-1}. The energy per pulse at ~5 μm was about 160 μJ [J. Y. Zhang, J. Y. Huang, Y. R. Shen, C. Chen, *J. Opt. Soc. Am. B* **10**, 1758 (1993)].
11. Because the photomultiplier had a cutoff beyond 850 nm, the spectra in Fig. 2, although normalized, may still be somewhat distorted.
12. P. Guyot-Sionnest, *Phys. Rev. Lett.* **67**, 2323 (1991).

13. V.P.K. thanks the Deutsche Forschungsgemeinschaft (DFG) for the Habilitationsstipendium. The work of the Berkeley group was supported by the Director, Office of Energy Research, Office of Basic Energy Sciences, Materials Sciences Division of the U.S. Department of Energy under contract DE-AC03-76SF00098.

24 March 1995; accepted 29 August 1995

Carbon Dioxide Uptake by an Undisturbed Tropical Rain Forest in Southwest Amazonia, 1992 to 1993

John Grace,* Jon Lloyd, John McIntyre, Antonio C. Miranda, Patrick Meir, Heloisa S. Miranda, Carlos Nobre, John Moncrieff, Jon Massheder, Yadvinder Malhi, Ivan Wright, John Gash

Measurements of carbon dioxide flux over undisturbed tropical rain forest in Brazil for 55 days in the wet and dry seasons of 1992 to 1993 show that this ecosystem is a net absorber of carbon dioxide. Photosynthetic gains of carbon dioxide exceeded respiratory losses irrespective of the season. These gains cannot be attributed to measurement error, nor to loss of carbon dioxide by drainage of cold air at night. A process-based model, fitted to the data, enabled estimation of the carbon absorbed by the ecosystem over the year as 8.5 ± 2.0 moles per square meter per year.

Most of the world's tropical forest is mature and undisturbed, and little is known about its carbon balance. Ecologists consider that in an unvarying environment, undisturbed ecosystems are in a steady state such that photosynthetic gains are balanced by respiratory losses due to death and decomposition. However, the terrestrial biosphere may be undergoing fertilization as a result of increasing concentrations of CO_2 coupled with higher deposition rates of nitrogen (*1*, *2*). If this is the case, undisturbed tropical forest may be a large sink of CO_2 because of its huge area (*3*), 10×10^{12} m^2. Now we report direct measurements of CO_2 flux over tropical rain forest in the Brazilian Amazon, to test the hypothesis that virgin forest sequesters carbon from the atmosphere.

We measured fluxes of CO_2, water vapor, and sensible heat over undisturbed forest (*4*) at Reserva Jaru, Rondonia, Brazil (10°04.84′S, 61°56.60′W), during the dry and wet seasons (September 1992 and April to June 1993, respectively). An eddy co-

J. Grace, J. McIntyre, P. Meir, J. Moncrieff, J. Massheder, Y. Malhi, Institute of Ecology and Resource Management, University of Edinburgh, Edinburgh EH9 3JU, UK.
J. Lloyd, Environmental Biology Group, Research School of Biological Sciences, Institute of Advanced Studies, Australian National University, Canberra ACT 2601, Australia.
A. C. Miranda and H. S. Miranda, Laboratorio de Ecologia, Universidade de Brasilia, Brasilia, Brazil.
C. Nobre, Instituto National de Pesquisas Espaciais–CPTECH, Caixa Postal 001, 12.630-000 Cachoera Paulista, São Paulo, Brazil.
I. Wright and J. Gash, Institute of Hydrology, Wallingford, OX10 8BB, UK.

*To whom correspondence should be addressed.

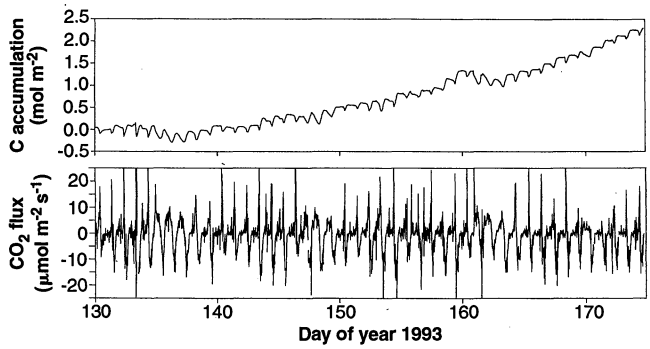

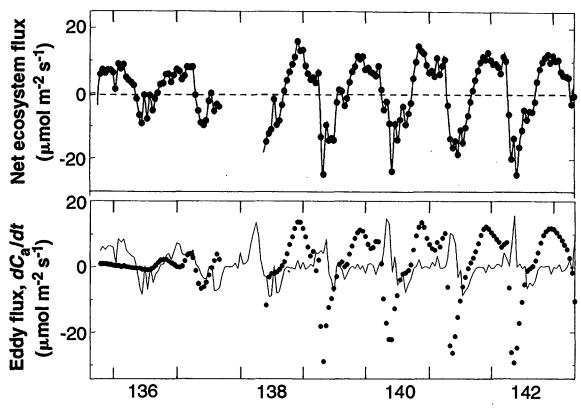

Fig. 1 (left). Eddy covariance data showing CO_2 fluxes over forest at Reserva Jaru for 44 days starting 9 May 1993, and their accumulated total. **Fig. 2 (right).** Examples of the diurnal cycles of net ecosystem CO_2 flux (top panel), obtained from the flux measured above the canopy (bottom panel, solid line) and the hourly changes in storage of CO_2 within the canopy air space (bottom panel, circles). Data are for the period 15 to 23 May (days 135 to 143).

variance system (*5*, *6*) mounted 15 m above the 30-m-tall forest was used to measure the fluxes over an area of about 1 km^2.

Each diurnal cycle of carbon flux shows net uptake during daylight of 5 to 20 μmol m^{-2} s^{-1} and a variable night-time efflux (Fig. 1). A feature of most days was a large spike of CO_2 leaving the canopy in the early morning. This spike was associated with the onset of turbulent conditions that followed calm nights and a corresponding decline in the concentration of CO_2 in the canopy as the air was flushed out. These spikes often exceeded 20 μmol m^{-2} s^{-1} sustained over 1 hour. There was considerable day-to-day variation in net (24-hour) flux, but 33 days out of 44 showed a downward net flux (from the atmosphere to the forest). The 11 days when the system lost carbon coincided with episodes of cool, cloudy, and windy weather in mid-May, 26 to 27 May, and 9 to 11 June. Accumulation of carbon over the 44-day period was 2.0 mol m^{-2} (Fig. 1). An error analysis, combining a possible 10% systematic and 10% random error on each half hour–averaged flux measurement, suggested an uncertainty of ±0.5 mol m^{-2}. A similar accumulation rate was observed at Jaru during the dry season (*7*).

To demonstrate the diurnal pattern of CO_2 assimilation and respiration of the forest, we added the hourly changes of in-canopy CO_2 storage (*8*) to the hourly above-canopy fluxes. The result shows that photosynthesis was maximal in the first part of the morning, well before the peak in solar irradiance (Fig. 2). By 16:00 the canopy was typically in a state of carbon balance; during the night, respiration was about 6.5 μmol m^{-2} s^{-1}. The data on night respiration were examined for a possible error in which CO_2 flux is "lost" when cold air drains away from a raised site (*9*). This effect was not detectable; moreover, the total night respiration measured was not significantly different from that estimated independently by chambers attached to the soil, stems, and leaves (*9*).

We related fluxes to diurnal changes in light, humidity, and temperature by fitting a model to the flux data (*10*). The model incorporates current understanding of turbulent transfer of CO_2 through the boundary layer (*11*), and diffusion of CO_2 through the stomata (*12*, *13*) and ultimately to the sites of carboxylation (*14*–*16*). Respiration from soil, stems, and branches was specified in this model with field data collected from the site (*17*). The model fitted the observations well (Fig. 3), and the plot of calculated carbon accumulation showed the same features as the actual carbon accumulation (Fig. 3, inset).

Using climatological data from the top of the observation tower (*18*), we then ran the model for a whole year (1 July 1992 to 30 June 1993). Over this period the model estimated a carbon accumulation of 8.5 ± 2.0 mol m^{-2} $year^{-1}$ for the area of rain forest examined. An earlier study in central Amazonia came to a similar conclusion (*7*). Such accumulation rates demonstrate the potential of the region to act as a carbon sink. If all the rain forest of the Amazon Basin (5×10^{12} m^2) were behaving in the same way as Reserva Jaru, the carbon accu-

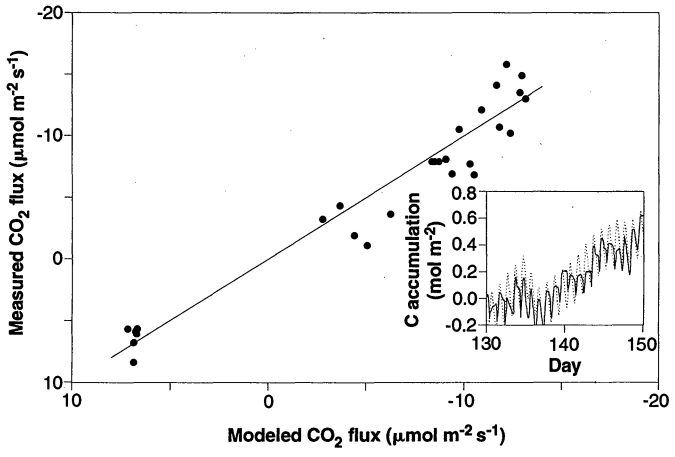

Fig. 3. Agreement between modeled and measured CO_2 fluxes. All data were selected to exclude periods of rapidly fluctuating solar radiation and wet weather, and wind directions from 170° to 260°. **(Inset)** Agreement between actual (solid line) and modeled (broken line) carbon accumulation.

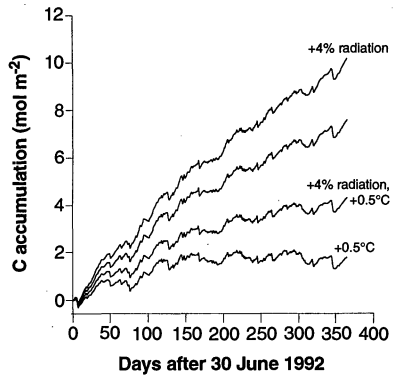

Fig. 4. Sensitivity analysis of the model. The model was run over an entire year, with 1-hour time steps, with the 1992 to 1993 climatological data as the standard run (this year was colder than usual, and may have been influenced by the eruption at Mount Pinatubo). Then the climatological input data were modified to explore the effect of increasing radiation and temperature, either separately or together. The run labeled +4% radiation, 0.5°C represents a best guess at an average year.

mulation in the Basin would be 45×10^{12} mol year^{-1} or 0.56 Pg year^{-1}. For comparison the Commonwealth Scientific and Industrial Research Organization–GASLAB flask experiment provides independent evidence that the whole of tropical South America may act as a carbon sink, by as much as 2 Pg per year in 1986 to 1987, but not in all years (*19*). Theoretical models of the effects of enhanced storage of carbon in terrestrial biomass as a result of increased CO_2 concentrations on net ecosystem fluxes predict a net influx of about 1 Pg year^{-1} for all of the tropics (*20, 21*).

Anthropogenic emissions of CO_2 amount to 5.7 Pg of carbon per year^{-1} as fossil fuel burning and about 2 Pg of carbon per year as deforestation (*22, 23*), whereas the annual increase in carbon as atmospheric CO_2 is only 3.5 Pg of carbon per year. It is presumed that the difference of about 4.2 Pg of carbon per year is distributed between the oceans and the terrestrial vegetation. Secondary forest, regrowth areas, and plantations are considered to be important candidates for terrestrial sinks (*24, 25*), but the present study suggests that the undisturbed forest may be more important. Year-to-year fluctuations in the carbon balance caused by climatic anomalies may be considerable, contributing to the interannual variation in the rate of CO_2 increase (*26*). For example, during 1992 to 1993 when our measurements were being made, the global environment may have been influenced by aerosols from the eruption of Mount Pinatubo, which reduced the solar irradiance by 4% and decreased the temperature by about 0.5°C (*27*). We investigated the sensitivity of the model to changes of this magnitude (Fig. 4). The result suggests great sensitivity to temperature. Part of the accumulated 8.5 mol of carbon per square meter of 1992 to 1993 may have been a result of cooler-than-normal temperatures in that year.

REFERENCES AND NOTES

1. C. Körner, in *Vegetation Dynamics and Global Change*, A. M. Solomon and H. H. Shugart, Eds. (Chapman & Hall, London, 1993), pp. 53–70.
2. R. M. Gifford, *Aust. J. Plant Physiol.* **21**, 1 (1994).
3. FAO, *Third Interim Report on the State of Tropical Forests* (FAO, Rome, 1992).
4. It is a palm-rich forest, classified as *Floresta Ombrofila Aperta*, with a leaf area index of about 4 and a height of 30 m. There is no evidence of human habitation or logging. The forest is on level terrain with good fetch.
5. R. Leuning and J. B. Moncrieff, *Boundary-Layer Meteorol.* **53**, 63 (1990).
6. A fast-responding closed-path gas analyzer was used to measure CO_2 and water vapor concentrations (Li 6262, Li-Cor, Lincoln, NE). Air from above the canopy (53 m above the ground, 20 m above the canopy) was drawn through 6-mm-diameter tubing (Dekabon 1300, Deane, Glasgow, UK) at a flow rate of 4 dm^3 min^{-1} into the gas analyzer. The calibration of the analyzer was checked every few days with a calibration cylinder prepared in our laboratory by means of precision gas-mixing pumps (Wosthoff OHG, Bochum, Germany). The vertical component of wind was measured at the same location with a three-dimensional sonic anemometer (A1012R, Gill Instruments, Lymington, UK). Fluxes were calculated as half-hour averages in real time with the software EdiSol, and the results were stored on a laptop computer. Corrections for the nonideal frequency response of the system were subsequently made; we expect the corrected signal to be within 10% of the true flux and to have a negligible zero offset.
7. Over 11 days in the dry season we obtained a mean accumulation rate of 0.09 mol m^{-2} day^{-1} compared with 0.05 mol m^{-2} day^{-1} in the wet season; S. Fan *et al* [*J. Geophys. Res.* **95**, 16851 (1990)] calculated an uptake of 0.05 mol m^{-2} day^{-1} over 50 days at a site near Manaus in central Amazonia.
8. For measurement of CO_2 storage in the canopy, vertical profiles were described by fitting spline curves to the CO_2 concentrations at 1, 15, 33, and 45 m; numerical integration from ground level to canopy-top gave the carbon stored in the canopy.
9. Mean nocturnal respiration measured from eddy covariance and CO_2 storage in the canopy was 6.6 μmol m^{-2} s^{-1} and did not decline with wind speed, as would be expected if loss due to drainage of cold air is important. The mean obtained independently from chamber methods (20 locations on the soil surface; and plant respiration measured at four heights in the canopy during night) was of similar magnitude, 7.2 ± 1.0 μmol m^{-2} s^{-1}.
10. To fit the model, we used a subset of the data: those values obtained when the leaves were dry, the radiation was not fluctuating, and the wind was not from the southern quarter (where the signal may have been contaminated by a river). At 25°C the fitted values were Rubisco activity 68 μmol m^{-2} s^{-1}, canopy electron transport of 130 μmol m^{-2} s^{-1}, and leaf respiration in the dark modeled as 0.7 μmol m^{-2} s^{-1}. The model is fully described in J. Lloyd *et al.*, *Plant Cell Envir.*, in press.
11. S. B. Verma, in *Estimation of Areal Evapotranspiration* (International Association of Hydrological Sciences, Wallingford, UK, 1989).
12. J. Lloyd *et al.*, *Austr. J. Plant Physiol.*, in press.
13. J. Lloyd, *ibid.* **18**, 649 (1991).
14. G. D. Farquhar *et al.*, *Planta* **149**, 78 (1980).
15. P. C. Harley *et al.*, *Oecologia* **70**, 393 (1986).
16. J. Lloyd *et al.*, *Plant Cell Envir.* **15**, 873 (1992).
17. Chambers were sealed to the soil surface, leaf, and stems, and fluxes were related to surface temperatures by an empirical equation.
18. Hourly data are collected with automatic weather stations at several forest towers in Brazil, as part of the Anglo-Brazilian Amazonian Climate Observation Study (ABRACOS) program.
19. I. G. Enting *et al.*, *Tellus* **47B**, 35 (1995).
20. P. J. Polglase and Y. P. Wang, *Aust. J. Bot.* **40**, 641 (1992).
21. J. A. Taylor and J. Lloyd (*ibid.* p. 407) and a recent theoretical study by J. Lloyd and G. D. Farquhar (*Funct. Ecol.*, in press) suggest that tropical forests are currently accumulating carbon in plant and soil at a rate of 5 to 8 mol m^{-2} year^{-1}.
22. R. A. Houghton, *Clim. Change* **19**, 99 (1991).
23. U. Siegenthaler and J. L. Sarmiento, *Nature* **365**, 119 (1993).
24. A. E. Lugo and S. Brown, *For. Ecol. Manage.* **54**, 239 (1992).
25. S. C. Wofsy *et al.*, *Science* **260**, 1314 (1993).
26. J. L. Sarmiento, *Nature* **365**, 697 (1993).
27. M. Blumthaler and W. Ambach, *Tellus* **46B**, 76 (1994).

28. We thank W. Coupland, I. Enting, P. Groeneveld, P. G. Jarvis, P. McCracken, A. McWilliam, and C. S. Wong for discussions and for practical help. We thank those organizations in Brazil that facilitated the field work: Instituto Nacional de Colonizacão e Reforma Agraria, Instituto Brasileiro de Meio Ambiente e Recursos Renováveis, Instituto Nacional de Pesquisas Espaciais, and University of Brasilia, Federal University of Rondonia. The ABRACOS project is supported by the UK Overseas Development Administration in collaboration with Agência Brasiliera de Cooperaçâo. The authors acknowledge the financial support provided by the Natural Environment Research Council through its TIGER (Terrestrial Initiative in Global Environment Research) program, award GST/02/605. J.L. was assisted by the Australia/New Zealand/UK Tripartate agreement on climate change.

11 May 1995; accepted 4 August 1995

Dynamic Contribution to Hemispheric Mean Temperature Trends

John M. Wallace, Yuan Zhang, James A. Renwick

On the basis of land station data from the Northern Hemisphere, it was determined that roughly half of the temporal variance of monthly mean hemispheric mean anomalies in surface air temperature during the period from 1900 through 1990 were linearly related to the amplitude of a distinctive spatial pattern in which the oceans are anomalously cold and the continents are anomalously warm poleward of 40 degrees north when the hemisphere is warm. Apart from an upward trend since 1975, to which El Niño has contributed, the amplitude time series associated with this pattern resembles seasonally dependent white noise. It is argued that the variability associated with this pattern is dynamically induced and is not necessarily an integral part of the fingerprint of global warming.

Much of the effort in the monitoring of hemispheric and global temperature trends is focused on the analysis of spatially averaged monthly time series such as the one presented in the top panel of Fig. 1 (*1*). The large month-to-month scatter inherent in such time series tends to obscure whatever interdecadal variability may be present, and it introduces large uncertainties into estimates of the current trends. It can be reduced by temporal smoothing, but only at the expense of the time resolution of the record. Here we show that most of this scatter can be identified with a distinctive spatial pattern of temperature fluctuations that is anchored to the land-sea distribution.

In the following, overbars denote spa-

Department of Atmospheric Sciences, Box 351640, University of Washington, Seattle, WA 98195–1640, USA.